Hyperfine Interact (2014) 224:179–188
DOI 10.1007/s10751-013-0857-y

Synthesis and characterization of uncoated and gold-coated magnetite nanoparticles

L. León-Félix · J. Chaker · M. Parise · J. A. H. Coaquira · L. De Los Santos Valladares · A. Bustamante · V. K. Garg · A. C. Oliveira · P. C. Morais

Published online: 22 March 2013

Abstract We report on the synthesis and characterization of uncoated and gold coated magnetite nanoparticles. Structural characterizations, carried out using X-ray diffraction, confirm the formation of magnetite phase with a mean size of ∼7 and ∼8 nm for the uncoated and gold covered magnetite nanoparticles, respectively. The value of the gold coated Fe_3O_4 nanoparticles is consistent with the mean physical size determined from transmission electron microscopy images. Mössbauer spectra at room temperature are consistent with the thermal relaxation of magnetic moments mediated by particle-particle interactions. The 77 K Mössbauer spectra are modeled with four sextets. Those sextets are assigned to the signal of iron ions occupying the tetrahedral and octahedral sites in the core and shell parts of the particle. The room-temperature saturation magnetization value determined for the uncoated Fe_3O_4 nanoparticles is roughly ∼60 emu/g and suggests the occurrence of surface effects such as magnetic disorder or the partial surface oxidation. These surface effects are reduced in the gold-coated Fe_3O_4 nanoparticles. Zero-field–cooled and

Proceedings of the Thirteenth Latin American Conference on the Applications of the Mössbauer Effect, (LACAME 2012), Medellín, Colombia, 11–16 November 2012.

L. León-Félix · M. Parise · J. A. H. Coaquira (✉) · V. K. Garg · A. C. Oliveira · P. C. Morais
Núcleo de Física Aplicada, Institute of Physics, University of Brasília, Brasília, DF 70910-900, Brazil
e-mail: coaquira.ja@gmail.com

J. Chaker
Faculdadede Ceilândia, University of Brasília, Brasília, DF 72220-140, Brazil

L. De Los Santos Valladares
Cavendish Laboratory, Department of Physics, University of Cambridge, J.J. Thomson Avenue, Cambridge CB3 0HE, UK

A. Bustamante
Laboratorio de Cerámicos y Nanomateriales, Facultad de Ciencias Físicas, Universidad Nacional Mayor de San Marcos, Ap. Postal 14-0149, Lima, Perú

field-cooled curves of both samples show irreversibilities which are consistent with a superparamagnetic behavior of interacting nanoparticles.

Keywords Au-coated magnetite nanoparticles · Mössbauer spectroscopy · Superparamagnetism

1 Introduction

Magnetite (Fe_3O_4) is one of the iron oxide phases of great interest for technological applications due to its high saturation magnetization, the highest ordering temperature among spinel ferrites and its low toxicity [1]. Magnetite nanoparticles (NPs) are interesting systems to be used in biomedical applications, bioseparation, magnetic recording media, target drug delivery, biochemical sensors, among others [2]. Therefore, the stability of iron oxide particles is impeded notably by the occurrence of spontaneous oxidation surface [3]. Recently, it has been revealed the possibility of surface passivation of magnetic nanoparticles (γ-Fe_2O_3, Fe_3O_4, Co, Fe, etc.) by a nonmagnetic shell (SiO_2, gold, silver, polymer, etc.) [4]. Core-shell structure of magnetic NPs is an attractive way to fabricate systems possessing unique physical and chemical properties [5]. Special attention has been given to gold (Au) NPs, since they show large surface area and suitable surface chemistry to be functionalized with thiolated molecules via covalent bonds [3]. Recently, core-shell gold coated magnetite NPs are reported to exhibit interesting optical properties (due to Au) and magnetic properties (due to Fe_3O_4) [5]. Therefore, Au-coated Fe_3O_4 NPs can provide a suitable platform for combine the magnetic properties of the iron oxide core with the gold shell which can be conjugated with biocompatible molecules in order to be used in biotechnological and biomedical applications.

It is known that bulk magnetite crystallizes in the cubic inverse spinel structure. The oxygen ions form a closed packed cubic structure with Fe ions localized in two different sites, octahedral and tetrahedral. Fe^{3+} ions occupy the tetrahedral sites (A) and Fe^{3+} and Fe^{2+} occupy octahedral sites (B) and are randomly arranged at room temperature because of an electron transfer process between these Fe^{3+} and Fe^{2+} ions. Below the $T_V \sim 125$ K, the electron hopping freezes out leading to an ordered array of Fe^{2+} and Fe^{3+} ions with static charge. This effect is manifested as a metal-insulator transition, which is known as the Verwey transition [6, 7]. That transition also modifies the magnetic properties and hyperfine interactions. Reports indicate that for untwined single crystals of magnetite, the low-temperature spectrum is composed of five sextets: one corresponds to Fe^{3+} ions at tetrahedral sites, two to Fe^{3+} ions at octahedral sites and two to Fe^{2+} ions at octahedral sites [8].

On the other hand, non-stoichiometric magnetite shows a reduced content of Fe^{2+} in octahedral sites. This non-stoichiometric magnetite stabilizes by the generation of cation vacancies at B sites. It is known that these vacancies screen the charge transfer and isolate the electron hopping process, since for each vacancy five Fe^{3+} ions in octahedral sites are trapped [6]. In Mössbauer spectrum these trapped Fe^{3+} ions at the octahedral sites and Fe^{3+} ions at the tetrahedral sites are indistinguishable without applying an external magnetic field [6]. Therefore, in a room-temperature Mössbauer spectrum of highly non-stoichiometric magnetite, the intensity transfer from $Fe_B^{2.5+}$ to Fe_A^{3+}-like component is observed. In this case, below

T_V the Mössbauer spectrum becomes strongly complicated. It is reported that the spectrum comprises a superposition of at least five components. For a small density of cation vacancies at B sites, the Verwey transition is shifted to lower temperatures and becomes less sharp (smoother) than in stoichiometric magnetite [6].

In the case of magnetite with reduced dimensionality, such as in nanoparticles, the surface or interface effects and particle-particle interactions strongly affect their hyperfine properties. It is difficult to distinguish between intrinsic size effects and effects related to deviation from the stoichiometry at the surface, driving to complicated Mössbauer spectra. Since at room temperature, Mössbauer spectrum shows features related to thermal relaxation, the models to fit the spectrum in order to determine the hyperfine parameters are not unique. A report suggests the use of single sextet to fit the room-temperature Mössbauer spectrum of magnetite NPs of ∼10 nm [9]. More recently publications on Mössbauer and magnetic study of magnetite NPs with a mean size of ∼8 nm reported the use up to 16 sextets in order to improve the fit quality of room-temperature Mössbauer spectra [10, 11].

Therefore, better knowledge of the magnetic, morphological and structural properties of coated magnetite nanoparticles is needed yet. In this work, we report the synthesis and characterization of uncoated and gold-coated Fe_3O_4 nanoparticles.

2 Experimental

The Fe_3O_4 nanoparticles were synthesized by the coprecipitation of Fe(II) and Fe(III) chlorides in aqueous solution. The solution was rinsing several times with distilled water and the black colored precipitation was collected by using a small magnet. Subsequently, 8 mL of Fe_3O_4 nanoparticles solution was added to 50 mL of 0.1 M sodium citrate and stirred at room temperature by ∼30 min to get the exchange absorbed OH^- with citrate anions [3]. In order to obtain the gold coated Fe_3O_4 nanoparticles, the latter solution was heated up to the boiling point by stirring vigorously. At this point, 2 μM of $HAuCl_4$ was slowly spilled into the nanoparticles solution and cooled by stirring [12]. The resultant material was washed with water and separated by high-speed ultra-centrifugation.

In order to determine the crystalline structure and estimate the mean crystallite size X-ray powder diffraction (XRD) was performed using a commercial diffractometer (Bruker, D8 advanced) with CuK_α radiation. Transmission electron microscopy (TEM) images were obtained by using a microscope (JOEL, model 1011) to determine the morphology, the mean particles size and the size distribution. Mössbauer spectroscopy (MS) measurements were carried out using a computer-controlled Wissel spectrometer with a triangular velocity mode and using a $^{57}Co(Rh)$ source with an activity of ∼20 mCi. A multichannel platform of 512 channels (before folding) has been used to register the spectra. 297 and 77 K spectra were obtained by cooling the sample in a commercial cryostat. A thin ∝-Fe foil has been used for calibration and a calibration error less than ∼0.5 % was estimated. The systematic error of unfolded spectrum is estimated to be ±0.02 mm/s. Thus, the velocity resolution and systematic error for hyperfine parameters should be ±0.04 mm/s for the 512-channels spectra and ±0.08 mm/s for 256-channels spectra. Isomer shifts are given related to ∝-Fe, at room temperature. All spectra were computer fitted with the least-square fitting routine using the NORMOS program and assuming

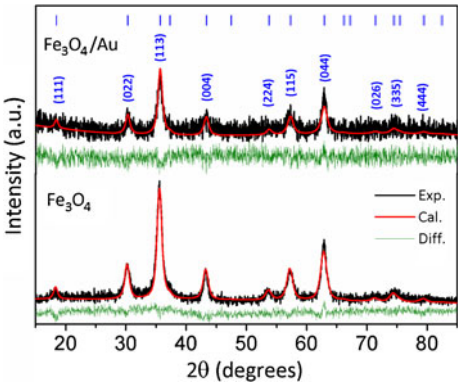

Fig. 1 Room temperature XRD patterns of the uncoated and gold-coated Fe_3O_4 nanoparticles. The observed and calculated data are represented by the *points* and *solid line*, respectively. The Bragg reflections are also indicated

Lorentzian lineshapes. The fit of Mösbauer spectra with a distribution of hyperfine fields has been carried out using the histogram method of the DIST subroutine of the NORMOS program, where the linewidth of each subspectrum is fixed to 0.3 mm/s. The magnetic properties were studied by magnetization measurements using the vibrating sample magnetometer (VSM) modulus of a physical property measurement system (PPMS) in a wide range of temperatures (from 5 to 340 K) and applying magnetic fields up to 90 kOe.

3 Results and discussion

Figure 1 shows the X-ray diffraction patterns of the uncoated and gold-coated Fe_3O_4 nanoparticles. As observed in the bottom part of Fig. 1, the Bragg reflections are consistent with the spinel structure of bulk magnetite (space group, $Fd\bar{3}m$). Although lower signal-to-noise ratio is obtained for the gold-coated Fe_3O_4 nanoparticles, no Bragg reflections corresponding to the Au crystalline phase have been determined and we assumed that the gold is located at the particle surface.

In order to estimate the particle size, XRD patterns have been refined by using the Rietveld method and modeling the peaks profile with a Pseudo-Voigt function. The particle size (D) is related to the linewidth (Γ) by the Scherrer equation: $D = 0.916\ \lambda/\Gamma \cdot \cos\theta_{hkl}$, where λ is the wavelength of the X-rays (0.15424 nm), and θ_{hkl} is the Bragg's angle [13]. The average crystallite sizes of $\langle D \rangle_{XRD} = (7.4 \pm 0.2)$ nm and (8.2 ± 0.2) nm are estimated for the uncoated and Au-coated NPs, respectively. The larger value obtained for the Au-coated NPs suggests that the gold covering process helps with the recrystallization of disordered regions likely present at the particle surface.

In order to corroborate these XRD results, TEM images were obtained. Figure 2 shows one of the TEM images obtained for the uncoated Fe_3O_4 NPs. With the help of the Imag-J software, several images have been used to count N ~ 1,000 particles. Subsequently, a particle size histogram has been mounted using the Sturges method [14]. The bin-width (W) is obtained from the relation: $W = (D_{max} - D_{min})/k$, where $k = 1 + 3.322 \log(N)$. That particle size histogram (see inset in Fig. 2) was modeled with a lognormal distribution: $f(D) = (1/\sqrt{2\pi}\ \sigma D) \exp\left[-\ln^2(D/D_0)/2\sigma^2\right]$, where D_0 is the median diameter and σ represents the degree of polydispersion. The mean value

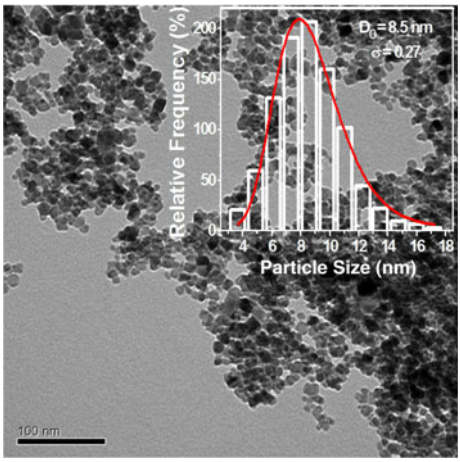

Fig. 2 TEM images of uncoated Fe_3O_4 NPs. In the inset is shown the histogram mounted as described in the text and modeled by a lognormal function

and its standard deviation are given by $< D >= D_0 e^{\sigma^2/2}$ and $\sigma_D =< D > \sqrt{e^{\sigma^2} - 1}$, respectively. Using those values, a mean particle size of $\langle D \rangle_{TEM} = (8.8 \pm 2.0)$ nm is estimated. TEM images (not shown here) obtained for the Au-coated Fe_3O_4 NPs show particle size consistent with the value obtained for the uncoated Fe_3O_4 NPs. Despite the large uncertainty, that mean value is in consistency to that obtained from XRD data of Au-coated NPs. This result implies that, after the gold surface covering, the crystalline size of the particle becomes comparable to the physical size. This result reinforces the finding that gold covering helps with the recrystallization of disordered regions likely formed at the particle surface.

Mössbauer spectra measured at room temperature and 77 K for the uncoated and Au-coated Fe_3O_4 NPs are shown in Figs. 3 and 4. At room temperature, thermal relaxation features related to the small particles size are observed. This relaxation drive to the starting collapse of magnetic sextets observed on both samples. These results are in agreement with magnetization data obtained near to 300 K (see below). In order to model the experimental data, the fit using a few number of sextets (for two sextets, one obtains a $\chi^2 \sim 1.81$) provides reasonable fits, but large linewidths ($\Gamma \sim 1.0$–2.0 mm/s). More plausible fits are obtained by using a distribution of hyperfine fields in which case a $\chi^2 \sim 1.03$ is obtained. The resultant histograms of the hyperfine field distribution are shown in Fig. 3. The broad distribution of hyperfine fields (from ~0 to 55 T) is in consistent with recent publications of Mössbauer spectroscopy results of magnetite nanoparticles with a mean size of ~8 nm, where the authors used a large number of sextets with hyperfine fields distributed in a broad range [11, 12].

The absence of a central doublet in the room temperature spectra of both spectra must be related to the strong particle-particle interaction and to the occurrence of magnetic correlations among the smallest particles. In order to compare the results obtained for both samples, the most probable component of the distribution is used. A most probable sextet with a hyperfine field of $B_{hf}^{\max} = (44.5 \pm 0.4)$ T, quadrupole shift of $2\varepsilon = (-0.02 \pm 0.08)$ mm/s and IS $= (0.36 \pm 0.08)$ mm/s are obtained for the uncoated NPs. Slightly different values are obtained for the Au-coated NPs ($B_{hf}^{\max} = (46.0 \pm 0.4)$ T, $2\varepsilon = (-0.00 \pm 0.08)$ mm/s and IS $= (0.38 \pm 0.08)$ mm/s).

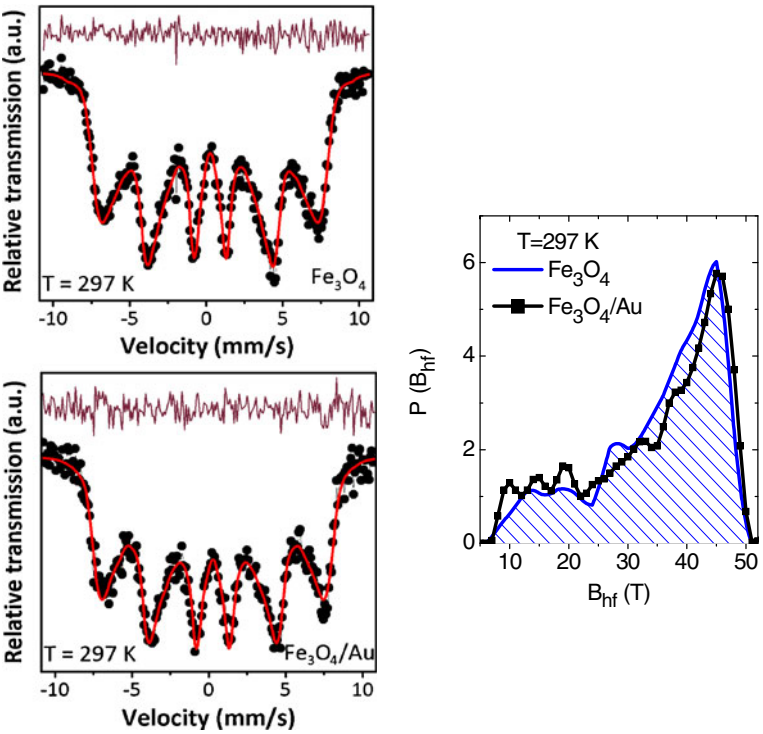

Fig. 3 Mössbauer spectra of Fe_3O_4 and Fe_3O_4/Au NPs obtained at room temperature. The points represent the experimental data and the *red line*, the calculated data. The difference between experimental and calculated data is shown at the top part of the plots. These spectra have been fitted using a distribution function of the hyperfine magnetic fields and the histograms are shown at the right-hand side

It suggests that the presence of gold ions at the particle surface slightly affects the particle-particle interaction, likely because of the partial surface coating.

At 77 K, the magnetic collapse is not else observed and the spectra of uncoated and Au-coated Fe_3O_4 NPs are well fitted by considering three sextets. $\chi^2 = 1.8$ and 2.5 are obtained for the Au-coated and the uncoated NPs, respectively. However, lower χ^2 are obtained (1.6 and 2.1 for the Au-coated and uncoated NPs, respectively) by considering four sextets (see Fig. 4). Fits considering more than five sextets provide lower χ^2, but unphysical values for the linewidth are obtained (<0.1 mm/s). As mentioned above, below 125 K, the electron transfer between Fe^{2+} and Fe^{3+} ions in B sites of bulk magnetite becomes slow and the presence of ferrous and ferric cations can be differentiated in the Mössbauer spectrum. Since it is difficult to distinguish between iron ions occupying tetrahedral or octahedral sites [8, 15], the origin of these sextets (S1, S2 and S3 components) are assigned to Fe^{3+} ions occupying both the tetrahedral and octahedral sites. Although the IS's for all sextets for uncoated NPs are the same within the experimental error the same, the lower hyperfine field and the larger linewidth of the S3 component suggest that this signal could come from the defective sites. The lowest hyperfine magnetic field of the S4 component could be assigned to iron ions located in the surface region of the

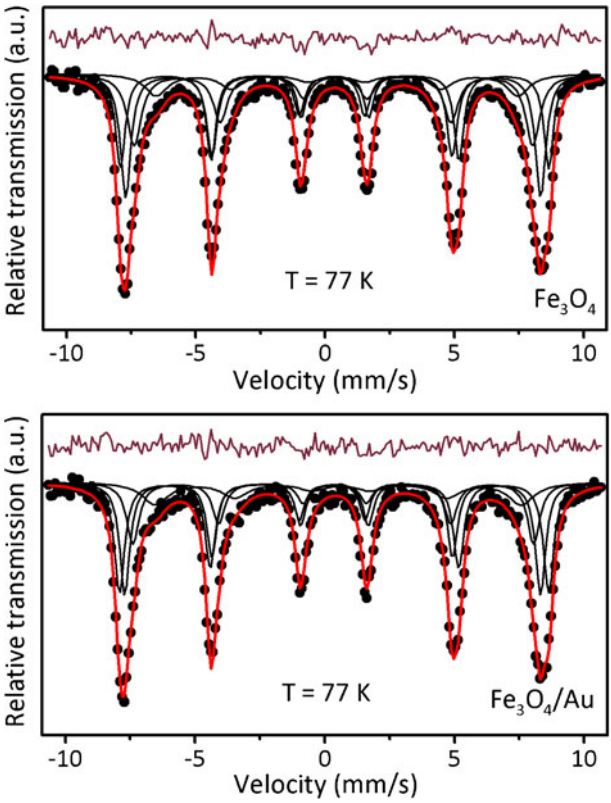

Fig. 4 Mössbauer spectra of Fe_3O_4 and Fe_3O_4/Au NPs obtained at 77 K. The *points* represent the experimental data and the *r*ed line represents the calculated data. The subspectra are also plotted as *c*ontinuous lines. The difference between experimental and calculated data is shown at the top part of the plots

particles. Within the experimental resolution, the spectral areas of all components (see Table 1) seem to remain the same in both samples. Although the spectral area of the S4 component seems to remain constant, the isomer shift shows a larger value for the Au-coated NPs. This increase in the IS could be assigned to the surface coating effects, since it seems that Au coating drives to the partial recrystallization of the particle surface. These results are preliminary and further study with more resolved Mössbauer spectroscopy measurements will permit to clarify this issue better.

Magnetizations (M) vs. magnetic field (H) curves have been obtained for both Fe_3O_4 and Fe_3O_4/Au NPs at 300 and 5 K. The M vs. H curves of uncoated and Au-coated NPs are shown in Fig. 5a. At 300 K, the saturation magnetization (Ms), determined by using the law of approach to saturation (a linear term is included in order to account for the linear increase of M at high fields), is found to be ~61 emu/g for the uncoated Fe_3O_4 NPs. This saturation magnetization value is consistent with the value reported in the literature for uncoated magnetite NPs of around the same mean size (~8 nm) [11]. Slightly larger value is obtained for the Fe_3O_4/Au NPs (~63 emu/g), which is consistent with the Mössbauer results as previously discussed. The increase of the saturation magnetization indicates that the Au covering of the NPs helps to reduce magnetically disordered regions, likely at the particle surface. Similar effects have been reported for surface-passivated magnetite nanoparticles which have been assigned to the improvement of the crystalline quality [11]. Moreover, those saturation magnetization values are significantly lower than the value

Table 1 List of hyperfine parameters, linewidths (Γ) and spectral areas (A) obtained from the fit of 77-K Mössbauer spectra of Fe_3O_4 and Au-coated Fe_3O_4

Sample	Site	IS (mm/s)	2ε (mm/s)	Bhf (T)	Γ (mm/s)	A (%)
Fe_3O_4	Fe^{3+} (S1)	0.48	−0.01	51.3	0.42	28
	Fe^{3+} (S2)	0.40	0.01	49.3	0.48	33
	Fe^{3+} (S3)	0.48	−0.02	47.8	0.66	27
	Fe′ (S4)	0.56	0.01	43.3	0.74	12
Fe_3O_4/Au	Fe^{3+} (S1)	0.47	−0.01	51.3	0.48	33
	Fe^{3+} (S2)	0.41	0.01	49.7	0.47	31
	Fe^{3+} (S3)	0.47	−0.05	47.9	0.56	21
	Fe″ (S4)	0.67	−0.10	43.8	0.70	15

The error of the spectral areas is estimated to be not more than 10 %

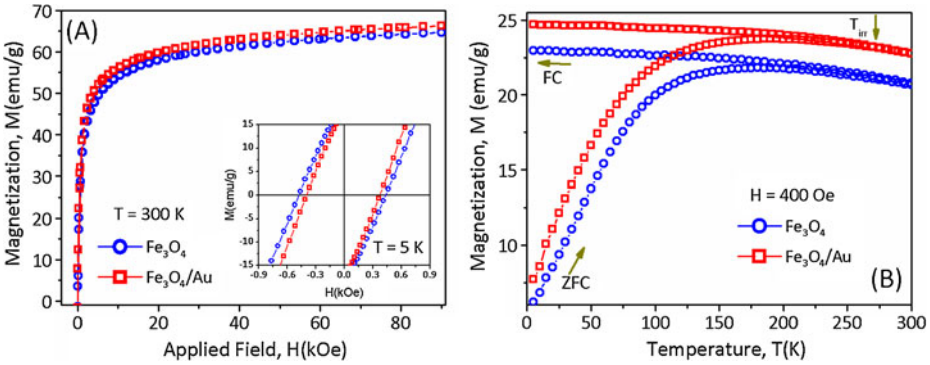

Fig. 5 **a** Hysteresis loops of Fe_3O_4/Au NPs at $T = 5$ K and room temperature. **b** Temperature dependence of zero-field-cooled (ZFC) and field-cooled (FC) curves of the Fe_3O_4 and Fe_3O_4/Au NPs

reported for bulk Fe_3O_4 (Ms ∼ 82 emu/g). These lower saturation magnetizations must be related to the surface effects [16, 17] or surface oxidation [6]. Those effects must be the responsible for the increasing tendency of the M vs. H curve observed in the high-field region.

At $T = 5$ K, the coercive field (H_C) determined for the uncoated Fe_3O_4 NPs is ∼460 while that determined for the Fe_3O_4/Au NPs is ∼390 Oe. The lower coercive field of the Fe_3O_4/Au NPs can be related to the recrystallization process of amorphous regions fulfilled by the gold shell covering the particles surface. Moreover, at 300 K, the coercive field of both samples decreases to $H_C \sim 12$ Oe. Since a zero coercive field is expected for the superparamagnetic behavior of small particles, the nonzero coercive field must be associated to the particle-particle interactions which delay the thermal relaxation of the magnetic moments of the particles [18].

Zero-field cooled (ZFC) and field cooled (FC) curves obtained with $H = 400$ Oe for the Fe_3O_4 and Fe_3O_4/Au NPs are shown in Fig. 5b. No evidences for the occurrence of the Verwey transition are observed in the temperature range from 5 to 300 K. The irreversible behavior of ZFC and FC curves reveals a typical thermal blocking process of superparamagnetic NPs. The ZFC curve shows a broad maximum at $T_m = 179 \pm 3$ K and 189 ± 3 K for the Fe_3O_4 and Fe_3O_4/Au NPs, respectively. In order to determine whether the studied samples can behave as superparamagnetic

systems, the magnetic particle size has been estimated. According to the Ref. [19] the mean magnetic sizes is given by: $D_{\mathrm{MAG}} = \left(18k_B T\chi_i/\pi\ \rho\ M_s^2\right)^{1/3}$, where $\chi_i = (\mathrm{dM/dH})_{H\to 0}$ is the initial susceptibility, k_B is the Boltzmann constant, Ms is the saturation magnetization and ρ is the mass density of magnetite. A value of $D_{\mathrm{MAG}} \sim 9$ nm, is obtained for both studied samples, which is in good agreement with the value obtained from XRD and TEM experiments. This result strongly suggests that the Fe_3O_4 NPs (uncoated and Au-coated) behave as weakly interacting entities. Therefore, the maximum of the ZFC curve can be related to the mean value of the blocking temperature (T_B). Considering a hypothetical system of monodispersed particles, then the relationship between these two temperatures is given by: $T_m = \beta\langle T_B\rangle$, where β is a parameter whose value is in the range of 1.4–1.6 [20]. Using $\beta = 1.5$ one can obtain $\langle T_B\rangle = 119 \pm 3$ K and $\langle T_B\rangle = 126 \pm 3$ K for the Fe_3O_4 and Fe_3O_4/Au NPs, respectively. The slightly larger T_B obtained for the Au-coated NPs, must be related to the larger particle size obtained from XRD and TEM data analysis.

One can estimate the anisotropy constant by using the relation $K_{\mathrm{an}} V\gamma = 25\, k_B T_B$, which is valid for a random distribution of a single domain magnetic particle. Here γ is a constant expected to be depend on the crystal size distribution ($\gamma = 9.2$) [21], K_{an} is the effective anisotropy constant and V is the volume the particle. Considering a $T_B \sim 120$ K and $D = 88$ nm for the uncoated NPs, an affective anisotropy constant of $K_{an} \sim 1.6 \times 10^5$ erg/cm^3 is determined. This value is close to that one reported in the literature for Fe_3O_4 NPs [22].

4 Conclusions

Structural characterization confirms the successful production of ~8-nm gold-coated Fe_3O_4 NPs. This mean particle size is corroborated by transmission electron microscopy. Room-temperature Mössbauer spectra of the uncoated and Au-coated Fe_3O_4 NPs are consistent with a distribution of magnetic particles which shows thermal relaxation of magnetic moments mediated by particle-particle interactions. However, at 77 K the Mössbauer spectra are well-modeled by four sextets, which are assigned to the signal of iron ions occupying tetrahedral and octahedral sites in the core and shell regions of the particles. The presence of gold on the particle surface produces effects which seem to be associated with the recrystallization of the shell region. Saturation magnetization values are lower than that of bulk magnetite and suggest the occurrence of surface effects which become important due to the large surface-to-volume ratio. The non-zero coercive field determined at room temperature indicates that the superparamagnetic behavior of NPs is mediated by the occurrence of particle-particle interactions.

Acknowledgements This work was financially supported by the Brazilian agencies CNPq and CAPES. JAHC thanks to DPP/UnB for the partial support.

References

1. Lima, Jr. E., Brandl, A.L., Arelaro, A.D., Goya, G.F.: J. Appl. Phys. **99**, 083908 (2006)

2. Zhou, X., Xu, W., Wang, Y., Kuang, Q., Shi, Y., Zhong, L., Zhang, Q.: J. Phys. Chem. C **114**, 19607 (2010)
3. Lyon, J.L., Fleming, D.A., Stone, M.B., Schiffer, P., Williams, M.E.: Nano Lett. **4**, 719 (2004)
4. Wu, W., He, Q., Chen, H., Tang, J., Nie, L.: Nanotechnology **18**, 145609 (2007)
5. Pal, S., Morales, M., Mukherjee, P., Srikanth, H.: J. Appl. Phys. **105**, 07B504 (2009)
6. Korecki, J., Handke, B., Spiridis, N., Slezak, T., Flis-Kabulska, I., Haber, J.: Thin Solid Films **412**, 14 (2002)
7. Voogt, F.C., Fujii, T., Smulders, P.J.M., Niesen, L., James, M.A., Hibma, T.: Phys. Rev B **60**, 11193 (1999)
8. Hargrove, R.S., Kündig, W.: Solid State Comm. **8**, 303 (1970)
9. Goya, G.F., Berquó, T.S., Fonseca, F.C., Morales, M.P.: J. Appl. Phys. **94**, 3520 (2003)
10. Oshtrakh, M.I., Sepelák, V., Rodriguez, A.F.R., Semionkin, V.A., Ushakov, M.V., Santos, J.G., Silveira, L.B., Marmolejo, E.M., De Souza Parise, M., Morais, P.C.: Spectrochim. Acta, Part A **100**, 94 (2013)
11. Oshtrakh, M.I., Ushakov, M.V., Semenova, A.S., Kellerman, D.G., Šepelák, V., Rodriguez, A.F.R., Semionkin, V.A., Morais, P.C.: Hyperfine Interact (2013). doi:10.1007/s10751-012-0666-8
12. Loaiza, Ó.A., Jubete, E., Ochoteco, E., Cabañero, G., Grande, H., Rodríguez, J.: Biosens. Biolectron. **26**, 2194 (2011)
13. Cullity, B.D., Stock, S.R.: Elements of X-ray Diffraction, 3rd edn. Prentice-Hall, Upper Saddle River, NJ (2001)
14. Aragón, F.H., de Souza, P.E.N., Coaquira, J.A.H., Hidalgo, P., Gouvêa, D.: Physica B **407**, 2601 (2012)
15. Presniakov, I.A., Sobolev, A.V., Baranov, A.V., Demazeau, G., Rusakov, V.S.: J. Phys., Condens. Matter **18**, 8943 (2006)
16. Gee, S.H., Hong, Y.K., Erickson, D.W., Park, M.H., Sur, J.C.: J. Appl. Phys. **93**, 7560 (2003)
17. Morales, M.P., Veintemillas Verdaguer, S., Montero, M.I., Serna, C.J., Roig, A., Casas, Ll., Martínez, B., Sandiumenge, F.: Chem. Mater. **11**, 3058 (1999)
18. Cho, S.-J., Idrobo, J.-C., Olamit, J., Liu, K., Browning, N.D., Kauzlarich, S.M.: Chem. Mater. **17**, 3181 (2005)
19. Carpenter, E.E.: J. Magn. Magn. Mater. **225**, 17 (2001)
20. Coaquira, J.A.H., Vaccari, C.B., Tedesco, A.C., Morais, P.C.: IEEE Trans. Magn. **45**, 4059 (2009)
21. Mikhaylova, M., Kim, D.K., Bobrysheva, N., Osmolowsky, M., Semenov, V., Tsakalakos, T., Muhammed, M.: Langmuir **20**, 2472 (2004)
22. Jonsson, T., Mattsson, J., Djurberg, C., Khan, F.A., Nordblad, P., Svedlindh, P.: Phys. Rev. Lett. **75**, 4138 (1995)